

Mirror symmetry rupture in double photoionization of endohedrally confined atoms

F. D. Colavecchia¹, G. Gasaneo², and D. Mitnik³

¹*Div. Colisiones Atómicas, Centro Atómico Bariloche and Conicet,
8400 S. C. de Bariloche, Río Negro, Argentina*

²*Departamento de Física, Universidad Nacional del
Sur and Conicet, 8000 Bahía Blanca, Argentina and*

³*Instituto de Astronomía y Física del Espacio,
Dep. de Física, Universidad de Buenos Aires,
and Conicet, 1428 Buenos Aires, Argentina*

(Dated: October 31, 2018)

Abstract

We study the double electronic emission by photon impact from He in the center of a spherical fullerene, which is modeled by a square-well shell. This system exhibits a manifold of avoided crossings as a function of the well depth, and present mirror collapses. However, this symmetry is broken in the triple differential cross section due to the delocalization of the He electrons in the initial state. Moreover, the fullerene potential involves higher angular momenta partial waves to be included in the process, which modifies the well-known two-lobe cross section from isolated He.

PACS numbers: 31.15.vj, 32.80.Fb, 37.30.+i

Fullerene molecules, formed by pentagonal and hexagonal arrangements of atoms, have received attention right from its discovery and undoubtedly opened many new captivating areas in physics. These molecules come in different sizes and shapes, from the well known, quasi spherical C_{60} carbon fullerene [1] to nanotubes. Beyond the specific features of fullerenes, many methods to include atoms inside their shells have been developed [2, 3]. These compounds form stable molecules that also attracted the interest of the community, such as their potential use as nanocages to storage atoms [4, 5]. Many properties of these systems are determined by the differences in the physics of the embedded atom compared to the isolated one.

Some of the most interesting of these features arise when these endohedrally embedded atoms interact with light and electronic emission occurs during the process. Since the pioneering work of Puska and Nieminen [6], different kinds of resonant behavior have been identified. First evidence of these effects were observed in the photoionization of C_{60} , revealed as oscillations in the cross sections [7] and attributed to the ability of the carbon shell to support an intramolecular standing wave. Confinement resonances are predicted for endohedrally embedded atoms such as $Xe@C_{60}$ [8, 9], due to the reflection of the photoelectron in the fullerene cage. Furthermore, the role of multielectronic correlation has been investigated recently, giving rise to the so-called correlation confinement resonances [10], and also the interference among resonances [11]. However, all these works involved a complex multielectronic atom inside the fullerene shell, that gives rise to many mechanisms of electronic emissions even when the atom is isolated.

Few works are devoted to multiple photoionization of fullerenes or endohedrally embedded atoms. Kidun et al. have examined the multiple photoionization of C_{60} within a many particle approach [12]. Two-electron photoionization has been studied for high photon energies by Amusia [13], but only the double-to-single photoionization cross sections ratio were reported. They analyzed the process with highly asymmetrical energy sharing, where the energy of one electron is much bigger than the energy of the other one. The emission in that case proceeds with a shake off mechanism, where the fast electron absorbs most of the energy of the photon, while the slow one is ejected due to the residual modified atomic field left after the ejection of the first one. Since their model of the fullerene potential was a delta function, it did not take into account accurately the possible delocalization of the atomic electrons into the cage.

Whereas the investigation of bound or continuum states of two electron systems can be performed by different techniques, double photoionization (DPI) of atomic or molecular species by single photons has unique advantages. First, it enables to directly probe the dynamics of the electron pair both in the initial and final states with the same collisional process. Besides, it is free of long-range correlations between the target and the incoming particles. Finally, the complete absorption of the photon by both electrons is determined by the interelectronic correlation. Then, it is not surprising that this process has been thoroughly studied along the years for both atomic and molecular species [14].

In this work we bring a different perspective to the problem of DPI from endohedrally embedded atoms. We choose the simplest system to study the role of the fullerene cage in the electronic emission, as well as the influence of the interelectronic correlation in the process, both in the bound state as well as in the continuum one. To this end, we consider a He atom in the center of the fullerene cage and assume that there are only two active electrons in the system. We also focus on equal energy sharing conditions for the ejected photoelectrons. The simplified electronic structure of the fullerene molecule seen by an electron has been usually described through a cage model potential [6]:

$$V_w(r) = \begin{cases} -U_0 & \text{if } r_c \leq r \leq r_c + \Delta \\ 0 & \text{otherwise} \end{cases} \quad (1)$$

For C_{60} , $r_c = 5.75$ a.u., $\Delta = 1.89$ a.u. [6, 7]. These simple assumptions enable one to discover all the richness of these systems. Moreover, different spherical fullerenes are described varying the well depth. In fact, the energetic structure of these molecules as a function of the magnitude of the cage potential U_0 presents a manifold of avoided crossing between states, even within this two-electron model [15, 16]. Similar results were found for endohedrally embedded hydrogen [17]. For the sake of simplicity, we choose to analyze the crossing between the ground and first excited states. Thus, the initial state of the system will be written in terms of one electron 1s ($\phi_{1s}(r) = 4\sqrt{2}\exp(-2r)$) and 2s ($\phi_{2s}(r) = 2\exp(-r)(1-r)$) states of the isolated atom, and the approximate solution of the model potential (1), $\phi_w(r) = \exp(-\alpha(r-r_0)^2)$ where $r_0 = r_c + \Delta/2$. We construct the following configuration interaction (CI) wave function with these one-electron wave functions for the

bound state:

$$\begin{aligned} \Psi_i(\mathbf{r}_1, \mathbf{r}_2) = N \{ & a \varphi_{1s}(r_1)\varphi_{1s}(r_2)\varphi_{corr}(r_{12}) \\ & + b [\varphi_{1s}(r_1)\phi_w(r_2) + 1 \leftrightarrow 2] \\ & + c [\varphi_{1s}(r_1)\varphi_{2s}(r_2) + 1 \leftrightarrow 2] \varphi_{corr}(r_{12}) \} \end{aligned} \quad (2)$$

where $\varphi_{corr}(r_{12}) = 1 + r_{12}/2$ is a correlation factor.

This state is suitable to analyze the collision process near the crossing between the ground and the first excited state of the system as a function of the potential depth. The basis parameters a, b, c as well as the exponential factor α , the normalization constant N and the energy depend on U_0 and are obtained with variational techniques, see Table 1. The crossing is at $U_0^{cross} = 1.35$ a.u.[18] We also choose two other values of the magnitude of the cage potential U_0 to calculate the cross sections, one below ($U_0 = 1.1$ a.u.) and one above ($U_0 = 1.65$ a.u.) the crossing of the levels. This particular selection of the basis does enhance the interplay between the free atomic ground state and the partially delocalized state with one electron in the atom and the other one in the fullerene, since the contribution of the $1s2s$ state through coefficient c is much smaller than the other ones. Thus, the basis parameters measure the degree of localization of the electrons: when $a \approx 1$, both electrons are near the atomic core, while $b \approx 1$ implies that the electronic density spreads up to the fullerene cage.

We assume a dipolar approximation for the DPI because usually experimental data is obtained in collisions with low energy photons [14]. The triply differential cross section (TDCS) in terms of the momenta \mathbf{k}_1 and \mathbf{k}_2 of the two ejected electrons can be obtained in the velocity gauge in terms of the transition matrix $T^{(V)}(\mathbf{k}_1, \mathbf{k}_2) = \langle \Psi_f^-(\mathbf{r}_1, \mathbf{r}_2) | \varepsilon \cdot (\nabla_1 + \nabla_2) | \Psi_i(\mathbf{r}_1, \mathbf{r}_2) \rangle$ where ε is polarization of the incoming light. We recall that this calculation can be performed also in acceleration or length gauges. Each gauge form emphasizes different regions of the configuration space, but all of them should give the same theoretical description of the process, provided that both the initial $\Psi_i(\mathbf{r}_1, \mathbf{r}_2)$ and final $\Psi_f^-(\mathbf{r}_1, \mathbf{r}_2)$ states are exact wave functions, or at least very good approximations for them. Otherwise, differences between gauges are apparent [19, 20]. For simple systems such as He, these differences are restricted to the magnitude of the cross sections, and minor deviations in the angular distributions [21] that are irrelevant for the mainly qualitative study presented here. The calculation of the transition matrix is performed by direct six-dimensional numerical integration in the

Table I: Energies and wave functions parameters (in atomic units) for ground and first excited states of He embedded in the model fullerene cage.

U_0	E	$N(\times 10^{-2})$	α	a	b	c
Ground State						
1.10	-2.8892	4.9390	0.47419	-0.99835	0.00187	0.05723
1.35	-2.9002	1.54985	0.54823	-0.94505	-0.31958	0.06879
1.60	-3.0905	0.54473	0.61216	-0.06843	-0.99762	-0.00798
First Excited State						
1.10	-2.7127	0.55145	0.47419	0.38490	-0.91623	0.11117
1.35	-2.8879	4.71427	0.54823	0.99770	-0.03930	-0.05509
1.60	-2.8890	4.94203	0.61216	0.99837	-0.00609	-0.05671

electronic spherical coordinates \mathbf{r}_1 and \mathbf{r}_2 , using a non-deterministic Vegas algorithm, with a relative error is smaller than 3% in the TDCS for all energies and angles considered[22].

Let us turn our attention to the final state of the ionized electrons in the continuum. Among many approximate wave functions for this state, we choose a simple C3-style wave function (See [23] and references therein):

$$\Psi_{C3}^{cage}(\mathbf{r}_1, \mathbf{r}_2) = \psi_{\mathbf{k}_1}^-(\mathbf{r}_1)\psi_{\mathbf{k}_2}^-(\mathbf{r}_2)D(\alpha_{12}, \mathbf{k}_{12}, \mathbf{r}_{12}) \quad (3)$$

where the electronic wave function in the combined field of the atomic core ($-2/r$) and the fullerene cage (V_w , eq.(1)) is described by the two-body functions $\psi_{\mathbf{k}_i}^-(\mathbf{r}_i)$ expanded in partial waves. For comparison purposes, we also make use of a pure Coulomb wave $\psi_{C3}^{Coul}(\mathbf{r}_1, \mathbf{r}_2)$, where the role of the cage potential is neglected. The electron-electron correlation is modeled with the usual Coulomb distortion factor $D(\alpha_{12}, \mathbf{k}_{12}, \mathbf{r}_{12}) = {}_1F_1(\alpha_{12}, 1, i\mathbf{k}_{12}\mathbf{r}_{12} + ik_{12}r_{12})$ in terms of the Sommerfeld parameter $\alpha_{12} = 1/k_{12}$ and the relative momentum $\mathbf{k}_{12} = \mathbf{k}_1 - \mathbf{k}_2$. This model correctly reproduces the asymptotic condition of the problem. We recall that, although this model would not lead to accurate absolute differential cross sections; it accounts for all the features of the collisional process for this system.

We computed emission in an equal energy sharing situation ($E_1 = E_2 = 10$ eV), with linearly polarized light. The calculations of TDCS as a function of the magnitude of the fullerene cage U_0 are displayed in Fig. 1. Overall, the cross sections interchange their

character as the states go through the avoided crossing, due to the mirror collapse of the initial state[16]. This is more evident for final Coulomb states (compare red lines in Fig. 1a with Fig. 1f; or Fig. 1d with Fig. 1c).

The emission from the ground state below the crossing (Fig. 1d) fully agrees with the isolated atom DPI from a $1s^2$ state as expected, and is similar for both final states used, $\psi_{C_3}^{Coul}(\mathbf{r}_1, \mathbf{r}_2)$ or $\psi_{C_3}^{cage}(\mathbf{r}_1, \mathbf{r}_2)$. Near and beyond the avoided crossing, the presence of the fullerene cage counteracts the interelectronic repulsion, moving the lobes towards the emission direction of electron 1 (Fig. 1d to Fig. 1f). This is slightly more important in the calculation that includes the cage in the final state (black curves in Fig. 1 online).

However, the excited state exhibits a more dramatic change along the crossing: the cross section changes from the typical two-lobe configuration to a four-lobe one. Thus, the mirror collapse observed in the initial state wave functions is broken in the cross sections. This effect can be clearly seen in Figs. 1a-c when compared with 1d-f, and it is present for both final states used, although it is noticeable at this energy only with the non-pure Coulomb final state $\psi_{C_3}^{cage}(\mathbf{r}_1, \mathbf{r}_2)$ at this emission energy. Both the initial and final states contribute to this feature. On one hand, the presence of a delocalized electron far from the nucleus in the initial state slightly changes the interelectronic repulsion. This has already been observed in calculations of double photoionization from He(1s2s) states [24], and were also attributed to the increasing extension of the initial state. On the other hand, the introduction of the cage potential in the final state $\psi_{C_3}^{cage}(\mathbf{r}_1, \mathbf{r}_2)$ plays a very important role, restraining the interelectronic repulsion (Fig. 1b) or enhancing it (Fig. 1c) for different well depths.

It is clear that the emission from the excited state deserves further investigation. The simple CI that we adopted to describe the initial state enables us to isolate the role of each CI state in the cross sections. We computed the contribution of each CI state separately for the DPI of the excited state, see Fig. 2. In this case, the energy sharing is $E_1 = E_2 = 50$ eV, and we choose a pure Coulomb wave $\psi_{C_3}^{Coul}(\mathbf{r}_1, \mathbf{r}_2)$ for the final state. Contribution of the CI atomic states results in the typical emission of electron 2 perpendicular to the direction of electron 1. However, the contribution of the atom-well CI state presents a complete different structure, with three clearly distinguishable lobes. It is clear from this figure that the shape of the cross section is mainly dictated by the *interplay* between CI states, and not by the simple superposition of them. This is clearly seen comparing Fig. 2a and 2c, where the contribution of the coherent sum determines the cross sections, while the role of

the interference among states clearly defines the behavior at the crossing, see Fig. 2b.

We can now compare the behavior of TDCS for different emission energies. While in Fig. 1b ($E_1 = E_2 = 10$ eV) two lobes are well defined when a pure Coulomb final wave is used, six lobes can be observed in Fig2b for $E_1 = E_2 = 50$ eV. This is not surprising, since the electronic density of the atom-well CI state has a maximum centered at the cage. Besides, partial waves with higher single electron angular momentum contribute to the cross section for increasing electron energies and are included in the process, which results in these structures in the cross sections. This is a unique effect due to the presence of the cage, because for isolated atoms, the centrifugal barrier inhibits the penetration of high angular momenta partial waves into the region where the atomic electronic density is significant. We have checked that this effect is enhanced when the final state $\Psi_{C_3}^{cage}(\mathbf{r}_1, \mathbf{r}_2)$ that includes the fullerene cage is used.

In summary, we have computed double photoionization cross sections from He endohedrally embedded in spherical fullerenes. This simple system shows striking differences with the electronic emission from isolated atoms. The presence of the fullerene cage determines the structure of the cross sections, breaking the initial state mirror collapse, and enhancing the role of higher angular momentum waves of the ejected electrons in the process. This effect is more remarkable for higher energies, although it can be seen for small ones, providing that the final state also includes the cage potential. The relation between the present results and other oscillatory properties found in this process deserves further explorations.

F. D. C. would like to acknowledge the financial support of ANPCyT (PICT 04/20548) and Conicet (PICT 5595). G. G. would like to acknowledge the support by PICTR 03/0437 of the ANPCYT (Argentina) and PGI 24/F038 of the Universidad Nacional del Sur (Argentina). D. M. acknowledges the support by UBACyT X471, of the Universidad de Buenos Aires (Argentina).

-
- [1] H. W. Kroto, J. R. Heath, S. C. O'Brien, R. F. Curl, and R. E. Smalley, *Nature* **318**, 162 (1985).
 - [2] D. S. Bethune, R. D. Johnson, J. R. Salem, M. S. de Vries, and C. S. Yannoni, *Nature* **366**, 123 (1993).

- [3] C. S. Yannoni, M. Hoinkis, M. S. de Vries, D. S. Bethune, J. R. Salem, M. S. Crowder, and R. D. Johnson, *Science* **256**, 1191 (1992).
- [4] O. V. Pupysheva, A. A. Farajian, and B. I. Yakobson, *Nano Letters* **8**, 767 (2008).
- [5] For a periodic table of endohedrally embedded atoms, see http://homepage.mac.com/jschrier/endofullerenes_table.html.
- [6] M. J. Puska and R. M. Nieminen, *Phys. Rev. A* **47**, 1181 (1993).
- [7] Y. B. Xu, M. Q. Tan, and U. Becker, *Phys. Rev. Lett.* **76**, 3538 (1996).
- [8] M. Y. Amusia, A. S. Baltenkov, and U. Becker, *Phys. Rev. A* **62**, 012701 (2000).
- [9] M. Y. Amusia, A. S. Baltenkov, V. K. Dolmatov, S. T. Manson, and A. Z. Msezane, *Phys. Rev. A* **70**, 023201 (2004).
- [10] V. K. Dolmatov and S. T. Manson, *J. Phys. B* **41**, 165001 (2008).
- [11] M. Y. Amusia, A. S. Baltenkov, and L. V. Chernysheva, *J. Phys. B* **41**, 165201 (2008).
- [12] O. Kidun, N. Fominykh, and J. Berakdar, *Comp. Mat. Science* **35**, 354 (2006).
- [13] M. Y. Amusia, E. Z. Liverts, and V. B. Mandelzweig, *Phys. Rev. A* **74**, 042712 (2006).
- [14] L. Avaldi and A. Huetz, *J. Phys. B* **38**, S861 (2005).
- [15] M. Neek-Amal, G. Tayebirad, and R. Asgari, *J. Phys. B* **40**, 1509 (2007).
- [16] D. M. Mitnik, J. Randazzo, and G. Gasaneo, *Phys. Rev. A* **78**, 062501 (2008).
- [17] J. P. Connerade, V. K. Dolmatov, P. A. Lakshmi, and S. T. Manson, *J. Phys. B* **32**, L239 (1999).
- [18] This value for the crossing depends on the model used for the initial state.
- [19] L. U. Ancarani, G. Gasaneo, F. D. Colavecchia, and C. Dal Cappello, *Phys. Rev. A* **77**, 062712 (2008).
- [20] A. S. Kheifets and I. Bray, *Phys. Rev. A* **69**, 050701(R) (2004).
- [21] S. P. Lucey, J. Rasch, C. T. Whelan, and H. R. J. Walters, *J. Phys. B* **31**, 1237 (1998).
- [22] T. Hahn, *Comp. Phys. Comm.* **168**, 78 (2005).
- [23] S. Otranto and C. R. Garibotti, *Phys. Rev. A* **67**, 064701 (2003).
- [24] J. Colgan and M. S. Pindzola, *Phys. Rev. A* **67**, 012711 (2003).

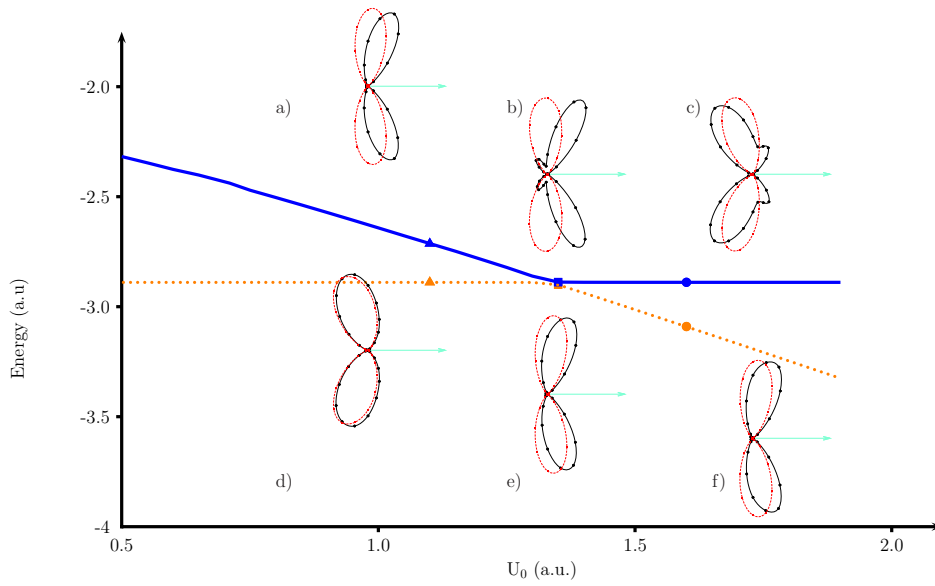


Figure 1: (Color online) Three fold differential cross section (TDCS) for $(\gamma, 2e)$ ionization of the helium ground state in a fullerene cage, as a function of the angle of one of the ejected electrons θ_2 . The other one is ejected at $\theta_1 = 0^\circ$, fixed respect to the polarization ε . The polarization vector is set along the \mathbf{x} axis, and the impinging light towards the page. The electrons are ejected with equal energy $E_1 = E_2 = 10$ eV. Dotted (orange) and solid (blue) lines represent the ground and excited state energy as a function of U_0 , respectively. TDCS are shown for both excited (a, b, c) and ground states (d, e, f); and computed with a pure Coulomb final state, dashed (red) line; or with exact potential including fullerene cage, solid (black) line. They are shown for $U_0 = 1.1$ a.u. (triangles), $U_0 = 1.35$ a.u. (squares) and $U_0 = 1.6$ a.u. (circles). All TDCS are rescaled to one at maxima.

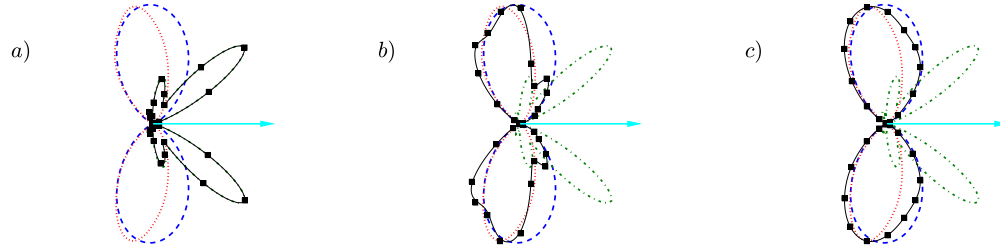


Figure 2: (Color Online) Contributions of the each initial CI states to the TDCS for $E_1 = E_2 = 50\text{eV}$, calculated with the pure Coulomb final state for the DPI of the excited state of endohedrally embedded He. Kinematics as well as values of U_0 are the same as in Fig. 1a)-1c). Solid (black online) line and squares: full TDCS, solid (cyan online) line, coherent contribution; dashed (blue) line, TDCS from first term, eq. (2); dash-dotted (green) line, TDCS from second term, eq (2); and dotted (red) line, TDCS from third term, eq. (2). All TDCS are rescaled to one at maxima.